HHS Public Access

Author manuscript

Nat Genet. Author manuscript; available in PMC 2016 July 11.

Published in final edited form as:

Nat Genet. 2016 February ; 48(2): 189–194. doi:10.1038/ng.3482.

Genome-wide association analysis identifies *TXNRD2, ATXN2* and *FOXC1* as susceptibility loci for primary open angle glaucoma

A full list of authors and affiliations appears at the end of the article.

Abstract

Primary open angle glaucoma (POAG) is a leading cause of blindness world-wide. To identify new susceptibility loci, we meta-analyzed GWAS results from 8 independent studies from the United States (3,853 cases and 33,480 controls) and investigated the most significant SNPs in two Australian studies (1,252 cases and 2,592 controls), 3 European studies (875 cases and 4,107 controls) and a Singaporean Chinese study (1,037 cases and 2,543 controls). A meta-analysis of top SNPs identified three novel loci: rs35934224[T] within *TXNRD2* (odds ratio (OR) = 0.78, P = 4.05×10^{-11} encoding a mitochondrial protein required for redox homeostasis; rs7137828[T] within *ATXN2* (OR = 1.17, P = 8.73×10^{-10}), and rs2745572[A] upstream of *FOXC1* (OR = 1.17, P = 1.76×10^{-10}). Using RT-PCR and immunohistochemistry, we show TXNRD2 and ATXN2 expression in retinal ganglion cells and the optic nerve head. These results identify new pathways underlying POAG susceptibility and suggest novel targets for preventative therapies.

Glaucoma is a clinically and genetically complex disease that is the leading cause of irreversible blindness worldwide[1,2]. Primary open-angle glaucoma (POAG), the most common form of the disease in most populations[3], is characterized by retinal ganglion cell apoptosis and progressive optic nerve damage[4]. While recent genome-wide association studies (GWAS) have identified interesting POAG risk loci[5–9], these account for only a fraction of disease heritability. To identify new POAG loci, we have completed a meta-analysis of GWAS summary findings of individuals of European descent from the United States with replication in an Australian study (ANZRAG) and further evaluation in a second Australian study (BMES), 3 European studies and a Singaporean Chinese dataset.

Correspondence: Janey L. Wiggs, ; Email: janey_wiggs@meei.harvard.edu

[55]A list of members and affiliations is provided in the Supplementary Note.

[*]These authors contributed equally

[#]These authors contributed equally.

Author Contributions

J.N.C.B., L.R.P., J.H.K., J.L.H, and J.L.W. were involved in designing the study. R.R.A., C.C.K., M.B., D.L.B., H.C., W.G.C., G.C., I.D.V., J.H.F., P.F., C.F., D.G., T.G., A.W.H., F.H., D.J.H., R.K.L., Z.L., P.R.L., D.A.M., P.M., P.M., S.E.M., S.A.P., Q.Q., T.R., J.E.R., P.M.R., E.R., R.R., J.S.S., W.K.S., K.S., A.J.S., R.M.T., F.T., A.C.V., D.V., G.W., T.Y.W., B.L.Y., D.J.Z., K.Z., N.W., B.W., R.N.W., M.A.P.-V., T.A., E.N.V., S.M., J.E.C., M.A.H., L.R.P., J.L.H., and J.L.W. were involved in participant recruitment, sample collection or genotyping. Analysis was performed by J.N.C.B., S.J.L., J.H.K., P.G., C.C.K., K.P.B., A.A.B., A.B., H.A., D.I.C., R.P.I., P.H., C.A.G., A.A-K., C.-Y.C., A.P.K., M.R., Y.E.S., S.S.V., J.J. W., K.S., C.J.H., P.K., L.R.P., S.M., J.L.H., and J.L.W. Designing and conducting the laboratory experiments were performed by K.W.P., Y.L., G.H., and J.L.W. Clinician assessments were performed by R.R.A., D.L.B., W.G.C., J.H.F., D.G., A.W.H., R.K.L., P.R.L., D.A.M., S.E.M., T.R., R.R., J.S.S., K.S., A.J.S., F.T., A.C.V., G.W., T.Y.W., D.J.Z., K.Z., J.E.C., L.R.P., and J.L.W. The initial draft was written by J.N.C.B., L.R.P. J.H.K., J.L.H. and J.L.W.

For stage 1 (discovery) we meta-analyzed summary data from 8 independent datasets (3,853 cases and 33,480 controls; Supplementary Table 1) with European ancestry from the United States collectively referred to as the National Eye Institute Glaucoma Human Genetics Collaboration Heritable Overall Operational Database (NEIGHBORHOOD). For all 8 NEIGHBORHOOD studies cases were primarily defined as at least 1 reliable visual field showing loss consistent with glaucoma, without a secondary cause, or CDR (cup-to-disc ratio) ≥ 0.7 or CDR asymmetry ≥ 0.2 or documented progression of optic nerve degeneration (in the Ocular Hypertension Treatment Study [OHTS])[10]. Controls had CDR <0.7. Additionally, for all datasets except OHTS, controls had intraocular pressure (IOP) of < 21 mmHg (Supplementary Table 2). For each dataset, site-specific quality control (sample and genotype call rates ≥ 95%), principal components analysis (EIGENSTRAT[11]), and imputation (IMPUTE2[12] or MACH[13,14]) were completed using the 1000 Genomes Project reference panel (March 2012) (Supplementary Note, Supplementary Table 3). Imputed variants with minor allele frequencies <5% or imputation quality scores (r2) <0.7 were removed prior to analysis. Dosage data, in the form of estimated genotypic probabilities, were analyzed in ProbABEL[15] for each dataset using logistic regression models, adjusting for age, sex, any significant eigenvectors and study-specific covariates. Genomic inflation was less than 1.05 (λ-value) for each individual dataset (Supplementary Figure 1). Estimated genotypic probabilities for 6,425,680 variants were meta-analyzed in METAL[16] using the inverse variance weighted method. To confirm that the results were not skewed by a particular dataset we completed a sensitivity analysis by selectively removing each dataset and meta-analyzing the remaining 7. The ORs from each grouping of 7 datasets were highly correlated with the results obtained from all 8 datasets (Supplementary Figure 2).

The stage 1 genome-wide association results are shown in Supplementary Figure 3, and the association results for all SNPs with $P < 1\times10^{-5}$ are shown in Supplementary Table 4. One SNP (rs2745572[A]) located in a novel region on 6p 50Kb 5′ of *FOXC1* reached genome-wide significance (OR = 1.25, $P = 2.36\times10^{-9}$) in stage 1 (Table 1). Additionally, 873 SNPs including SNPs located in regions not previously associated with POAG on 1p, 2p, 2q, 5p, 6p, 6q, 10q, 12q, 20p, and 22p had $P< 1\times10^{-5}$ (Supplementary Table 4).

Next we investigated the associations of the most significant stage 1 SNPs ($P< 1\times10^{-5}$) in a replication dataset of European Caucasians from Australia (ANZRAG, Australian and New Zealand Registry of Advanced Glaucoma; 1,155 cases and 1,992 controls) (Supplementary Note), and performed a meta-analysis of these SNPs in the NEIGHBORHOOD and ANZRAG datasets using the effect sizes and their standard errors (stage 2). In the meta-analysis, SNPs in novel regions 50kb 5′ of *FOXC1* [top SNP rs2745572[[A], OR = 1.23, $P = 6.5\times10^{-11}$], within intron 14 of *ATXN2* [top SNP rs7137828 [T], OR = 1.18, $P = 9.2\times10^{-9}$] and within intron 11 of *TXNRD2* [top SNP rs35934224[T], OR = 0.77, $P = 1.8\times10^{-9}$] reached genome-wide significance (Table 1, Supplementary Table 5). The regional association results for these SNPs are shown in Figure 1.

For each of the 3 novel regions reaching genome-wide significance after stage 2, we further examined their association with POAG in: a second Australian dataset (BMES, Blue Mountains Eye Study) (107 cases and 600 controls); 3 European datasets (875 cases and 4,107 controls in total); and a study of Singaporean Chinese (1,037 cases and 2,543

controls); (stage 3). Meta-analysis of all datasets exceeded genome-wide significance for all three top SNPs (Figure 2, Supplementary Figure 4): *TXNRD2* rs35934224[T], combined P = 4.05×10^{-11}, OR = 0.78; *ATXN2* rs7137828[T], combined P = 4.40×10^{-10}, OR = 1.17; and *FOXC1* rs2745572[A], combined P = 1.76×10^{-10}, OR = 1.17 (Supplementary Tables 6 and 7). The *ATXN2* top SNP (rs7137828) is very rare in the Singaporean Chinese population and thus could not be evaluated.

SNPs in the *GAS7* region, previously associated with intraocular pressure (IOP), a quantitative trait that, when elevated, is a risk factor for glaucoma[17–19], were significantly associated with POAG after stage 2 (top SNP rs9897123[T], OR = 0.83, P = 5.85×10^{-10}) (Table 1). Other POAG loci identified in recent studies[5–9] were also confirmed, including *TMCO1, CDKN2BAS, SIX6, ABCA1*, and *AFAP1* (Table 1, Supplementary Table 8). *PMM2* SNPs recently identified in Chinese POAG[9] were nominally associated with POAG (top SNP rs12444233[T], OR = 1.13, P = 0.0016).

POAG, like many complex human diseases, displays clinical sub-phenotypes[20,21]. In particular, optic nerve degeneration in POAG can occur without elevation of IOP, a clinical subtype defined as normal-tension glaucoma (NTG)[22]. The NEIGHBORHOOD POAG dataset included 725 NTG cases (maximum IOP ≤ 21 mm Hg) and 1,868 high tension glaucoma (HTG) (maximum IOP > 21 mm Hg) cases (pretreatment IOP was not available for 1260 cases). The meta-analysis of NTG cases (using all the controls from the datasets with NTG cases) revealed one novel locus on chromosome 12q (rs2041895 [C], OR= 1.48, P = 2.41×10^{-8}) in stage 1 (Supplementary Figure 5, Supplementary Table 9). The direction of effect was consistent (OR=1.15) in the ANZRAG NTG dataset, but did not reach significance (P=0.11) and the combined association result (NEIGHBORHOOD + ANZRAG) fell just short of genome-wide significance (P= 8.01×10^{-8}), possibly due to a smaller number of NTG cases in the ANZRAG dataset (N=363). In the NEIGHBORHOOD discovery dataset we confirmed previous NTG associations on 9p[7] (*CDKN2BAS* top SNP rs1333037[T], OR = 1.67, P=1.35×10^{-12}) and 8q22[7] (top SNP, rs284491[T], OR = 0.66, P=2.30×10^{-8}) and in the HTG subgroup, (1,868 cases) confirmed associations with *TMCO1*[6,17], and *SIX6*[7,23] (Supplementary Figure 6, Supplementary Table 10). The *FOXC1* region SNPs associated with POAG overall were also significant in the NEIGHBORHOOD HTG subgroup (most significant SNP rs2317961, OR =0.76, P = 2.58×10^{-8}).

To assess the possible functional effects of SNPs at the three newly identified POAG loci, we accessed and applied data from ENCODE[24], SCAN (eQTL)[25], GENEVAR (eQTL)[26], GTEx (eQTL)[27] and RegulomeDBv2[28,29]. After stage 2, seven SNPs reached genome-wide significance in the *FOXC1* region (Supplementary Table 5) and all seven of these are located 50Kb 5′ to *FOXC1* in a region annotated by ENCODE as regulatory (Supplementary Figure 7) and are associated with enhancers in several cell types (P=0.01, RegulomeDBv2). The most significant SNP (rs2745572) is evolutionarily conserved (GERP = 1.8) and alters a Barhl1 transcription factor binding site (RegulomeDBv2). In zebrafish Barhl1 is expressed in distinct retinal cell lineages and is differentially regulated by Atoh7[30], a retinal-specific transcription factor that has been previously associated with optic nerve area[31] and glaucoma[32]. In the NEIGHBORHOOD meta-analysis we found nominal evidence for association with *ATOH7* and POAG (top SNP rs1867567[A] P = 0.042, OR, 1.07).

Four SNPs in the *ATXN2* region were significantly associated with POAG after stage 2 (Supplementary Table 5). These SNPs are located in genomic regions enriched for enhancers (P = 0.01) in lymphoid cells (RegulomeDBv2). The most significant SNP (rs7137828) is located in a SP1 transcription factor binding site, and another associated SNP, rs653178 which is in linkage disequilibrium with rs7137828 (R^2>0.8, Caucasian European Ancestry) is located in an Esr2 (Estrogen receptor 2) binding site. Both SP1 and Esr2 are expressed in retinal cells[33, 34] and could influence expression of *ATXN2*[35].

The *TXNRD2* region that includes 22 associated SNPs at the genome-wide level after stage 2 (Supplementary Table 5) is significantly enriched for enhancers ($P=1\times10^{-6}$, RegulomeDBv2) and DNaseI hypersensitivity sites ($P = 4.3\times10^{-5}$, RegulomeDBv2) in multiple cell types. Additionally, 6 of the *TXNRD2* SNPs are cis eQTLs significantly affecting *TXNRD2* transcript levels in MuTHer (Multiple Tissue Human Expression Resource) Twins[36] in lymphoblasts and skin ($P=1\times10^{-8}$, GENEVAR; Supplementary Figure 8). The top SNP (rs35934224) is also an eQTL in skin using RNA seq and 1000 Genomes imputation ($P=2.32\times10^{-13}$)[37]. All 22 *TXNRD2* SNPs are significant cis eQTLs ($P<1\times10^{-4}$) in the GTEx database[27] in thyroid tissue and 19 are significant eQTLs in tibial nerve tissue (Supplementary Figure 9). The most significant *TXNRD2* SNP (rs35934224) is located in a binding site for NRSF (neuron-restrictive silencer factor, also known as REST, (repressor element 1-silencing transcription factor), a transcription factor that potently protects neurons from oxidative stress[38].

FOXC1 is a member of the forkhead family of transcription factors and rare coding sequence mutations (missense, nonsense, and CNVs) are known to cause anterior segment dysgenesis and early-onset glaucoma with dominant inheritance[39,40]. *FOXC1* has not been previously implicated in common adult-onset forms of glaucoma including POAG or HTG. Interestingly, association over *GMDS*, located 3′ to *FOXC1*, has been identified in a study using some of the same samples used here[8]. In our study we found genome-wide significant association adjacent to *FOXC1* in the 5′ regulatory region and less significant association in *GMDS* (top SNP rs9378638, OR = 0.83, $P = 7.50\times10^{-6}$). The top SNPs in the two regions are approximately 400kb apart and are not in linkage disequilibrium. Conditional analysis confirmed that the odds ratio and P-value for the significantly associated SNPs 5′ to *FOXC1* are unchanged by conditioning on the *GMDS* peak SNP, suggesting that these are independent associations (Supplementary Figure 10). The 5′ regulatory SNPs associated with POAG and HTG identified by this study could be involved in regulation of *FOXC1* expression.

The *ATXN2* and *TXNRD2* genomic regions have not been previously associated with POAG or with any glaucoma-related quantitative traits such as optic nerve parameters or IOP. Expansions of an *ATXN2* CAG repeat can cause spinocerebellar ataxia 2 with optic atrophy and intermediate expansions can contribute to development of amyotrophic lateral sclerosis (ALS)[41]. Interestingly, very recently two other genes known to be responsible for Mendelian forms of NTG have also been shown to contribute to ALS (amyotrophic lateral sclerosis)[42,43]. The *ATXN2-SH3* region has been associated with retinal venular caliber in Caucasians with European ancestry[44]. We analyzed the expression of *ATXN2* mRNA in normal human ocular tissues by RT-PCR and found expression in the cornea, trabecular

meshwork, ciliary body, retina and optic nerve (Supplementary Figure 11). Immuno-labeling of sections of a normal mouse eye showed evidence of Atxn2 in the retinal ganglion cells and optic nerve (Figure 3).

TXNRD2 codes for thioredoxin reductase 2, a mitochondrial protein necessary for reducing damaging reactive oxygen species generated by oxidative phosphorylation and other mitochondrial functions[45]. Cellular oxidative stress has been hypothesized as a cause of retinal ganglion cell dysfunction in glaucoma[46] and over-expression of thioredoxin 2, the substrate of thioredoxin reductase 2 (encoded by *TXNRD2*), increased retinal ganglion cell survival in an experimental glaucoma model[47]. We confirmed by RT-PCR that *TXNRD2* is expressed in normal human ocular tissue (Supplementary Figure 11) including the retina and optic nerve. Immuno-labeling in mice showed strong staining in retinal ganglion cells as well as in the optic nerve (Figure 3). These data suggest that reduction of reactive oxygen species by *TXNRD2* could prevent mitochondrial dysfunction and retinal ganglion cell apoptosis in glaucoma. *TXNRD2* is the first mitochondrial protein associated with glaucoma risk.

In this study, common variants near *FOXC1, ATXN2* and *TXNRD2* were identified as new risk loci for POAG. These genes suggest novel pathways that may contribute to glaucoma development including abnormal ocular development (*FOXC1*), neuro-degeneration (*ATXN2*) and mitochondrial dysfunction secondary to accumulating reactive oxygen species (*TXNRD2*). Targeting these pathways could lead to effective and potentially preventative glaucoma therapies.

URLS

ENCODE, http://www.genome.gov/encode/ and http://genome.ucsc.edu/ENCODE/

GENEVAR, http://www.sanger.ac.uk/resources/software/genevar/

GTEx, http://www.gtexportal.org/home/

IMPUTE, http://mathgen.stats.ox.ac.uk/impute/impute.html

LocusZoom, (http://csg.sph.umich.edu/locuszoom/)

MACH, http://csg.sph.umich.edu/abecasis/MACH/download/

METAL, http://csg.sph.umich.edu/abecasis/metal/index.html

NEIGHBORHOOD, http://glaucomagenetics.org

ProbABEL, http://www.genabel.org/

RegulomeDBv2, http://www.broadinstitute.org/mammals/haploreg/haploreg.php

SCAN, http://www.scandb.org/

SHAPEIT, https://mathgen.stats.ox.ac.uk/genetics_software/shapeit/shapeit.html

1000 Genomes Project, http://www.1000genomes.org/

Data access

Summary data for the NEIGHBORHOOD POAG meta-analysis is available on the NEIGHBORHOOD website (URL listed above, see 'Publications').

Online Methods

Study design

Imputed genotypes (1000 Genomes panel, March 2012) for 3,853 cases and 33,480 controls from 8 independent datasets were used as the discovery cohort for this genome-wide association study for Primary Open Angle Glaucoma (POAG) (stage 1). The association results for the top SNPs from the discovery cohort were replicated in 1,155 cases and 1,992 controls from an Australian POAG study of Caucasians of European ancestry (stage 2) followed by further replication (stage 3) in a second Australian study, BMES (Blue Mountains Eye Study) and 3 European studies (EPIC (European Prospective Investigation into Cancer-Norfolk Eye Study), GER (Germany), UK (United Kingdom); (982 cases and 4,707 controls total), and a Singaporean Chinese datasest of 1,037 cases and 2,543 controls. The details for all datasets including genotyping platforms, quality control, imputation methods and diagnostic criteria are listed in the Supplementary Notes.

Meta-analysis (Discovery, stage 1)

Quality-control was performed for each data set as described in the Supplementary Note. Overall sample and genotype call rates were ≥ 95% for each site. Samples with Log R ratio (LRR) and B allele frequency (BAF) values suggestive of copy number variants were removed prior to analysis. Principal components (eigenvectors) were computed for all participants using EIGENSTRAT[11]. For each dataset logistic regression was performed in ProbABEL[15] for all analyses (POAG overall, HTG, NTG), controlling for age, sex, and study-specific covariates including study-specific eigenvectors. Each analysis was evaluated separately for overall genomic inflation (implementing the R package GenABEL) (λ-value ≤ 1.05 for each dataset) (Supplementary Figure 1). Results were meta-analyzed in METAL[16] implementing the inverse variance weighted method and applying genomic control correction.

Replication (Stage 2 and 3)

Loci of interest in the discovery cohort (NEIGHBORHOOD; $P<1\times10^{-5}$) were evaluated in the first replication cohort (ANZRAG) and meta-analyzed with the NEIGHBORHOOD results (stage 2). The top SNPs for the three novel regions were evaluated in 5 additional datasets, one Australian (BMES), 3 European (EPIC, GER, UK) and a Singaporean Chinese dataset.

Power calculations

Power calculations were done as described[48]. For the stage 1 discovery analysis, power calculations using disease prevalence of 2%[49] indicated that there was 96% power of detecting loci at $P < 1.0 \times 10^{-5}$ (the threshold for carrying over to stage 2) at minor allele frequencies as low as 30% with per-allele odds ratios of 1.17. The entire sample set (stages

1, 2 and 3) had 99% power to detect loci at $P < 5.0 \times 10^{-8}$ at minor allele frequencies as low as 30% with per-allele odds ratios as low as 1.17.

Candidate genes and functional effects

Genes of interest in the associated region were identified using Ensembl[50], UCSC genome Bioinformatics[51], and Genecards[52]. To predict functional effects of the top POAG associated SNPs, we used the ENCODE project data[24], HaploReg v2[28] and RegulomeDB[29]. We used SCAN[25], Genevar[26] and GTEx[27] and a study of UK twins using RNA seq and 1000 genomes imputation[37] to investigate expression quantitative trait loci within genomic regions of interest.

Statistical analyses

Conditional analyses were done using the top SNPs in the *FOXC1, ATXN2*, and *TXNRD2* regions as well as the top SNP in the previously reported *GMDS* region[8] conditioning on the risk allele in the region of interest. Conditional analyses were performed using GCTA (Genome Complex Trait Analysis)[53].

Forest plots to visualize the effect sizes of top SNPs in each region by dataset were created using the rmeta package in R. The odds ratios and 95% confidence intervals for each displayed SNP were plotted and the P-values listed for each analysis (Figure 2) and each NEIGHBORHOOD dataset (Supplementary Figure 4).

Sensitivity analysis using the leave-one-out method was done by excluding each NEIGHBORHOOD dataset from a meta-analysis of the other 7 datasets. We compared the odds ratios from these analyses by calculating the Pearson's product-moment correlation coefficient between each leave-one-out analysis and the overall meta-analysis of eight NEIGHBORHOOD datasets (Stage 1), as shown in Supplementary Figure 2. Correlations were calculated in R using the corrplot package and ellipse option.

Expression analysis of genes at associated loci in ocular tissues

Total RNA was extracted from dissected tissues from normal human donor eyes as previously described[54,55] using an RNA isolation kit from Life Technologies (Carlsbad, CA, USA). Reverse Transcriptional reactions were completed using SuperScript III reverse transcriptase from Life Technologies. Primer sequences were designed to specifically amplify *TXNRD2* and *ATXN2*. PCR reactions were performed using the recommended conditions with Platinum Taq DNA polymerase (Life Technologies, Carlsbad, CA, USA) using a Touch Down program. Amplified PCR products were visualized by gel electrophoresis with 2% agarose gel.

Immunohistochemistry

C57BL/6J mice (males and females) were maintained on a 12/12 hours light/dark cycle. All experiments were approved by the Animal Care and Use Committee at The Jackson Laboratory. Eyes from 2–4 months old C57BL/6J mice were enucleated and fixed in 4% Paraformaldehyde for 2 hours, rinsed in 0.1M Phosphate buffer, immersed in 30% sucrose overnight and frozen in OCT. 15 mm sections were placed on Fisherbrand Superfrost Plus

Slides and stored at −70°C until required. Sections were incubated overnight at 4°C in the following primary antibodies: rabbit anti TXNRD2 (1:50 Acris); rabbit anti-ATXN2 (1:50, Acris). All antibodies were diluted in PBT (1×PBS, 1% TritonX-100). Sections were blocked in 2.5% chicken serum (in PBT) for 1 hour, then incubated overnight at 4oC. After primary incubation, sections were washed 3 times in PBT and incubated with the secondary antibody (goat anti-rabbit IgG) for 4hrs at 4°C. All sections were then counterstained with DAPI and mounted with Aqua PolyMount. Images were collected on a Leica SP5 Confocal microscope. For each antibody, at least 3 sections from 6 eyes were assessed. Antibodies were obtained from Acris: Ataxin 2, Catalogue number: 21776-1 AP; Immunogen: Ag16470; Genebank ID (clone info): BC114546; Purification method: Antifen affinity purification; Txnrd2: Catalogue number: 16360-1-AP; Immunogen: Ag8367; Genebank ID (clone info): BC007489; Purification method: Antifen affinity purification.

All images in Figure 3 were taken on a Leica SP5 confocal microscope. Images in left and center panels were taken with a 20× glycerol objective, right panels were taken with a 63× glycerol objective. Excitation was performed using a 405 Diode laser (DAPI) and Argon laser (ATXN2 or TXNRD2). Collection was performed using sequential scanning: scan 1 = PMT 1 (gain 966) for DAPI, scan 2 = PMT 2 (gain 1013) for ATXN2 or TXNRD2.

Supplementary Material

Refer to Web version on PubMed Central for supplementary material.

Authors

Jessica N. Cooke Bailey[1,*], Stephanie J. Loomis[2,*], Jae H. Kang[3], R. Rand Allingham[4], Puya Gharahkhani[5], Chiea Chuen Khor[6,7], Kathryn P. Burdon[8,9], Hugues Aschard[10], Daniel I. Chasman[11], Robert P. Igo Jr.[1], Pirro G. Hysi[12], Craig A. Glastonbury[12], Allison Ashley-Koch[13], Murray Brilliant[14], Andrew A. Brown[15], Donald L. Budenz[16], Alfonso Buil[15], Ching-Yu Cheng[7,17,18], Hyon Choi[19], William G. Christen[11], Gary Curhan[3,20], Immaculata De Vivo[3], John H. Fingert[21,22], Paul J. Foster[23,24], Charles Fuchs[3,25], Douglas Gaasterland[26], Terry Gaasterland[27], Alex W. Hewitt[28,29], Frank Hu[10,30], David J. Hunter[10,31], Anthony P. Khawaja[32], Richard K. Lee[33], Zheng Li[6], Paul R. Lichter[34], David A. Mackey[8,35], Peter McGuffin[36], Paul Mitchell[37], Sayoko E. Moroi[34], Shamira A. Perera[17,38], Keating W. Pepper[39], Qibin Qi[40], Tony Realini[41], Julia E. Richards[34,42], Paul M Ridker[11], Eric Rimm[3,10,30], Robert Ritch[43], Marylyn Ritchie[44], Joel S. Schuman[45], William K. Scott[46], Kuldev Singh[47], Arthur J. Sit[48], Yeunjoo E. Song[1], Rulla M. Tamimi[3], Fotis Topouzis[49], Ananth C. Viswanathan[23], Shefali Setia Verma[44], Douglas Vollrath[50], Jie Jin Wang[37], Nicole Weisschuh[51], Bernd Wissinger[51], Gadi Wollstein[45], Tien Y. Wong[7,17], Brian L. Yaspan[52], Donald J. Zack[53], Kang Zhang[54], EPIC-Norfolk Eye Study[55], ANZRAG consortium[55], Robert N. Weinreb[54], Margaret A. Pericak-Vance[46], Kerrin Small[12], Christopher J. Hammond[12], Tin Aung[17,18], Yutao Liu[56,57], Eranga N. Vithana[17,18], Stuart MacGregor[5], Jamie E. Craig[9], Peter Kraft[10,31], Gareth Howell[39], Michael A. Hauser[4,13], Louis R. Pasquale[2,3], Jonathan L. Haines[1,#], and Janey L. Wiggs[2,#]

Affiliations

[1]Department of Epidemiology and Biostatistics, Institute for Computational Biology, Case Western Reserve University School of Medicine, Cleveland, OH [2]Department of Ophthalmology, Harvard Medical School, Massachusetts Eye and Ear Infirmary, Boston, MA [3]Channing Division of Network Medicine, Brigham and Women's Hospital, Harvard Medical School, Boston, MA [4]Department of Ophthalmology Duke University Medical Center, Durham, NC [5]QIMR Berghofer Medical Research Institute, Brisbane, Queensland, Australia [6]Division of Human Genetics, Genome Institute of Singapore [7]Department of Ophthalmology, Yong Loo Lin School of Medicine, National University of Singapore [8]Menzies Institute for Medical Research, University of Tasmania, Hobart, TAS, Australia [9]Department of Ophthalmology, Flinders University, Adelaide, SA, Australia [10]Department of Epidemiology, Harvard School of Public Health, Boston, MA [11]Division of Preventive Medicine, Brigham and Women's Hospital, Harvard Medical School, Boston, MA [12]Department of Twin Research and Genetic Epidemiology, King's College London, London, UK [13]Department of Medicine, Duke University Medical Center, Durham, NC [14]Center for Human Genetics, Marshfield Clinic Research Foundation, Marshfield, WI [15]Department of Genetic Medicine and Development, University of Geneva Medical School, Geneva, Switzerland [16]Department of Ophthalmology, University of North Carolina, Chapel Hill, NC [17]Singapore Eye Research Institute, Singapore National Eye Centre, Singapore [18]Eye Academic Clinical Program, Duke-National University of Singapore Graduate Medical School, Singapore [19]Section of Rheumatology and Clinical Epidemiology Unit, Boston University School of Medicine, Boston, MA [20]Renal Division, Department of Medicine, Brigham and Women's Hospital, Boston, MA [21]Department of Ophthalmology University of Iowa, College of Medicine, Iowa City, IO [22]Department of Anatomy and Cell Biology, University of Iowa, College of Medicine, Iowa City, IO [23]National Institute for Health Research Biomedical Research Centre at Moorfields Eye Hospital [24]Department of Ophthalmology, University of Cambridge, London [25]Department of Medical Oncology, Dana-Farber Cancer Institute, Harvard Medical School, Boston, MA [26]Eye Doctors of Washington, Chevy Chase, MD [27]Scripps Genome Center, University of California at San Diego, San Diego, CA [28]Centre for Eye Research Australia, University of Melbourne, Australia [29]Royal Victorian Eye and Ear Hospital, Melbourne, Victoria, Australia [30]Department of Nutrition, Harvard School of Public Health, Boston, MA [31]Program in Genetic Epidemiology and Statistical Genetics, Harvard School of Public Health, Boston, MA [32]Department of Public Health and Primary Care, Institute of Public Health, University of Cambridge School of Clinical Medicine, Cambridge, UK [33]Bascom Palmer Eye Institute University of Miami Miller School of Medicine, Miami, FL [34]Department of Ophthalmology and Visual Sciences, University of Michigan, Ann Arbor, MI [35]Centre for Ophthalmology and Visual Science, Lions Eye Institute, University of Western Australia, Perth, Western Australia, Australia [36]Medical Research Council Social Genetic and Developmental Psychiatry Research Centre, Institute of Psychiatry, King's College, London, UK [37]Centre for Vision Research, Westmead Millennium Institute, University of Sydney,

Westmead, New South Wales, Australia [38]Duke-National University of Singapore Graduate Medical School, Singapore [39]The Jackson Laboratory, Bar Harbor, ME [40]Department of Epidemiology and Population Health, Albert Einstein College of Medicine, Bronx, NY [41]Department of Ophthalmology, West Virginia University Eye Institute, Morgantown, WV [42]Department of Epidemiology, University of Michigan, Ann Arbor, MI [43]Einhorn Clinical Research Center, Department of Ophthalmology, New York Eye and Ear Infirmary of Mt. Sinai, New York, NY [44]The Center for Systems Genomics, The Pennsylvania State University, University Park, PA [45]Department of Ophthalmology, University of Pittsburgh, Pittsburgh, PA [46]Institute for Human Genomics, University of Miami Miller School of Medicine, Miami, FL [47]Department of Ophthalmology, Stanford University School of Medicine, Palo Alto, CA [48]Department of Ophthalmology, Mayo Clinic, Rochester, MN [49]Department of Ophthalmology, School of Medicine, Aristotle University of Thessaloniki, AHEPA Hospital, Thessaloniki, Greece [50]Department of Genetics, Stanford University School of Medicine, Palo Alto, CA [51]Institute for Ophthalmic Research, Centre for Ophthalmology, University of Tübingen, Germany [52]Genentech, San Francisco, CA [53]Wilmer Eye Institute, Johns Hopkins University Hospital, Baltimore, MD [54]Hamilton Glaucoma Center, Shiley Eye Institute, University of California, San Diego, CA [56]Department of Cellular Biology and Anatomy, Georgia Regents University, Augusta, GA [57]James & Jean Culver Vision Discovery Institute, Georgia Regents University, Augusta, GA

Acknowledgments

The NEIGHBORHOOD data collection and analysis is supported by NIH/NEI R01EY022305 (JL Wiggs). Support for recruitment of ANZRAG (Australian and New Zealand Registry of Advanced Glaucoma) was provided by the Royal Australian and New Zealand College of Ophthalmology (RANZCO) Eye Foundation and by the National Health and Medical Research Council (NHMRC) of Australia (#535074, #1031362 and #1023911, #1021105). EPIC-Norfolk infrastructure and core functions are supported by grants from the Medical Research Council (G1000143) and Cancer Research UK (C864/A14136). BMES (Blue Mountains Eye Study) was supported by the NHMRC, Canberra Australia, the Centre for Clinical Research Excellence in Translational Clinical Research in Eye Diseases, NHMRC Senior Research Fellowships and the Wellcome Trust, UK. The South London Case-Control cohort (UK) collection and genotyping was supported by a National Institute of Health Research (NIHR) Senior Research Fellowship (CJ Hammond), and analysis was supported by a Fight for Sight Early Career Investigator Award (PJ Hysi). The Singapore study of EN Vithana, T Aung, and CC KHor, was supported by a Biomedical Research Council (BMRC) grant in Singapore, Ref: BMRC 10/1/35/19/675. This research was also partly supported by a grant (NMRC/TCR/008-SERI/2013) from the Singapore National Research Foundation under its Translational and Clinical Research Flagship Programme and administered by the Singapore Ministry of Health's National Medical Research Council. Additional acknowledgment and funding details are in the Supplementary Note.

References

1. Quigley HA, Broman AT. The number of people with glaucoma worldwide in 2010 and 2020. Br J Ophthalmol. 2006; 90:262267.
2. Tham YC, et al. Global prevalence of glaucoma and projections of glaucoma burden through 2040: a systematic review and meta-analysis. Ophthalmology. 2014; 121:2081–2090. [PubMed: 24974815]
3. Wang YX, Xu L, Yang H, Jonas JB. Prevalence of glaucoma in North china: the Beijing Eye Study. Am J Ophthalmol. 2010; 150:917–924. [PubMed: 20970107]

4. Weinreb RN, Aung T, Medeiros FA. The pathophysiology and treatment of glaucoma: a review. JAMA. 2014; 311:1901–1911. [PubMed: 24825645]
5. Thorleifsson G, et al. Common variants near CAV1 and CAV2 are associated with primary open-angle glaucoma. Nat Genet. 2010; 42:906–909. [PubMed: 20835238]
6. Burdon KP, et al. Genome-wide association study identifies susceptibility loci for open angle glaucoma at TMCO1 and CDKN2B-AS1. Nat Genet. 2011; 43:574–578. [PubMed: 21532571]
7. Wiggs JL, et al. Common variants at 9p21 and 8q22 are associated with increased susceptibility to optic nerve degeneration in glaucoma. PLoS Genet. 2012; 8:e1002654. [PubMed: 22570617]
8. Gharahkhani P, et al. Common variants near ABCA1, AFAP1 and GMDS confer risk of primary open-angle glaucoma. Nat Genet. 2014; 46:1120–1125. [PubMed: 25173105]
9. Chen Y, et al. Common variants near ABCA1 and in PMM2 are associated with primary open-angle glaucoma. Nat Genet. 2014; 46:1115–1119. [PubMed: 25173107]
10. Feuer WJ, et al. Ocular Hypertension Treatment Study Group. The Ocular Hypertension Treatment Study: reproducibility of cup/disk ratio measurements over time at an optic disc reading center. Am J Ophthalmol. 2002; 133:19–28. [PubMed: 11755836]
11. Price AL, et al. Principal components analysis corrects for stratification in genome-wide association studies. Nat Genet. 2006; 38:904–909. [PubMed: 16862161]
12. Howie BN, Donnelly P, Marchini J. A flexible and accurate genotype imputation method for the next generation of genome-wide association studies. PLoS genetics. 2009; 5:e1000529. [PubMed: 19543373]
13. Howie B, Fuchsberger C, Stephens M, Marchini J, Abecasis GR. Fast and accurate genotype imputation in genome-wide association studies through pre-phasing. Nat Genet. 2012; 44:955–959. [PubMed: 22820512]
14. Fuchsberger C, Abecasis GR, Hinds DA. minimac2: faster genotype imputation. Bioinformatics. 2015; 31:782–784. [PubMed: 25338720]
15. Aulchenko YS, Struchalin MV, van Duijn CM. ProbABEL package for genome-wide association analysis of imputed data. BMC Bioinformatics. 2010; 11:134. [PubMed: 20233392]
16. Willer CJ, Li Y, Abecasis GR. METAL: fast and efficient meta-analysis of genomewide association scans. Bioinformatics. 2010; 26:2190–2191. [PubMed: 20616382]
17. van Koolwijk LM, et al. Common genetic determinants of intraocular pressure and primary open-angle glaucoma. PLoS Genet. 2012; 8:e1002611. [PubMed: 22570627]
18. Ozel AB, et al. Genome-wide association study and meta-analysis of intraocular pressure. Hum Genet. 2014; 133:41–57. [PubMed: 24002674]
19. Hysi PG, et al. Genome-wide analysis of multi-ancestry cohorts identifies new loci influencing intraocular pressure and susceptibility to glaucoma. Nat Genet. 2014; 46:1126–1130. [PubMed: 25173106]
20. Gorlova O, et al. Identification of novel genetic markers associated with clinical phenotypes of systemic sclerosis through a genome-wide association strategy. PLoS Genet. 2011; 7:e1002178. [PubMed: 21779181]
21. Woo D, et al. Meta-analysis of genome-wide association studies identifies 1q22 as a susceptibility locus for intracerebral hemorrhage. Am J Hum Genet. 2014; 94:511–521. [PubMed: 24656865]
22. Anderson DR, Drance SM, Schulzer M, Collaborative Normal-Tension Glaucoma Study Group. Natural history of normal-tension glaucoma. Ophthalmology. 2001; 108:247–253. [PubMed: 11158794]
23. Carnes MU, et al. Discovery and functional annotation of SIX6 variants in primary open-angle glaucoma. PLoS Genet. 2014; 10:e1004372. [PubMed: 24875647]
24. ENCODE Project Consortium. A user's guide to the encyclopedia of DNA elements (ENCODE). PLoS Biol. 2011; 9:e1001046. [PubMed: 21526222]
25. Gamazon ER, et al. SCAN: SNP and copy number annotation. Bioinformatics. 2010; 26:259–262. [PubMed: 19933162]
26. Yang TP, et al. Genevar: a database and Java application for the analysis and visualization of SNP-gene associations in eQTL studies. Bioinformatics. 2010; 26:2474–2476. [PubMed: 20702402]

27. The GTEx Consortium. The Genotype-Tissue Expression (GTEx) pilot analysis: Multitissue gene regulation in humans. Science. 2015; 348:648–660. [PubMed: 25954001]
28. Ward LD, Kellis M. HaploReg: a resource for exploring chromatin states, conservation, and regulatory motif alterations within sets of genetically linked variants. Nucleic Acids Res. 2012; 40:D930–D934. [PubMed: 22064851]
29. Boyle AP, et al. Annotation of functional variation in personal genomes using RegulomeDB. Genome Res. 2012; 22:1790–1797. [PubMed: 22955989]
30. Schuhmacher LN, Albadri S, Ramialison M, Poggi L. Evolutionary relationships and diversification of barhl genes within retinal cell lineages. BMC Evol Biol. 2011; 11:340. [PubMed: 22103894]
31. Macgregor S, et al. Genome-wide association identifies ATOH7 as a major gene determining human optic disc size. Hum Mol Genet. 2010; 19:2716–2724. [PubMed: 20395239]
32. Chen JH, et al. Interactive effects of ATOH7 and RFTN1 in association with adult-onset primary open-angle glaucoma. Invest Ophthalmol Vis Sci. 2012; 53:779–785. [PubMed: 22222511]
33. Donovan K, Alekseev O, Qi X, Cho W, Azizkhan-Clifford J. O-GlcNAc modification of transcription factor Sp1 mediates hyperglycemia-induced VEGF-A upregulation in retinal cells. Invest Ophthalmol Vis Sci. 2014; 55:7862–7873. [PubMed: 25352121]
34. Mabuchi F, et al. Estrogen receptor beta gene polymorphism and intraocular pressure elevation in female patients with primary open-angle glaucoma. Am J Ophthalmol. 2010; 149:826–830. [PubMed: 20399928]
35. Sun Z, et al. Conserved recurrent gene mutations correlate with pathway deregulation and clinical outcomes of lung adenocarcinoma in never-smokers. BMC Med Genomics. 2014; 7:32–43. [PubMed: 24894543]
36. Grundberg E, et al. Mapping cis- and trans-regulatory effects across multiple tissues in twins. Nat Genet. 2012; 44:1084–1089. [PubMed: 22941192]
37. Buil AB, et al. Transcriptome sequencing reveals widespread gene-gene and gene-environment interactions. Nat Genet. 2015; 47:88–91. [PubMed: 25436857]
38. Lu T, et al. REST and stress resistance in ageing and Alzheimer's disease. Nature. 2014; 507:448–454. [PubMed: 24670762]
39. Ito YA, Goping IS, Berry F, Walter MA. Dysfunction of the stress-responsive FOXC1 transcription factor contributes to the earlier-onset glaucoma observed in Axenfeld-Rieger syndrome patients. Cell Death Dis. 2014; 5:e1069. [PubMed: 24556684]
40. D'haene B, et al. Expanding the spectrum of FOXC1 and PITX2 mutations and copy number changes in patients with anterior segment malformations. Invest Ophthalmol Vis Sci. 2011; 52:324–333. [PubMed: 20881294]
41. Lattante S, et al. Contribution of ATXN2 intermediary polyQ expansions in a spectrum of neurodegenerative disorders. Neurology. 2014; 83:990–995. [PubMed: 25098532]
42. Cirulli ET, et al. Exome sequencing in amyotrophic lateral sclerosis identifies risk genes and pathways. Science. 2015; 347:1436–1441. [PubMed: 25700176]
43. Freischmidt A, et al. Haploinsufficiency of TBK1 causes familial ALS and fronto-temporal dementia. Nat Neurosci. 2015; 18:631–636. [PubMed: 25803835]
44. Ikram MK, et al. Four novel Loci (19q13, 6q24, 12q24, and 5q14) influence the microcirculation in vivo. PLoS Genet. 2010; 6:e1001184. [PubMed: 21060863]
45. Chen Y, Cai J, Jones DP. Mitochondrial thioredoxin in regulation of oxidant-induced cell death. FEBS Lett. 2006; 580:6596–6602. [PubMed: 17113580]
46. Chrysostomou V, Rezania F, Trounce IA, Crowston JG. Oxidative stress and mitochondrial dysfunction in glaucoma. Curr Opin Pharmacol. 2013; 13:12–25. [PubMed: 23069478]
47. Caprioli J, Munemasa Y, Kwong JM, Piri N. Overexpression of thioredoxins 1 and 2 increases retinal ganglion cell survival after pharmacologically induced oxidative stress, optic nerve transection, and in experimental glaucoma. Trans Am Ophthalmol Soc. 2009; 107:161–165. [PubMed: 20126492]
48. Purcell S, Cherny SS, Sham PC. Genetic Power Calculator: design of linkage and association genetic mapping studies of complex traits. Bioinformatics. 2003; 19:149–150. [PubMed: 12499305]

49. Tham YC, Li X, Wong TY, Quigley HA, Aung T, Cheng CY. Global prevalence of glaucoma and projections of glaucoma burden through 2040: a systematic review and meta-analysis. Ophthalmology. 2014; 121:2081–2090. [PubMed: 24974815]
50. Flicek P, et al. Ensembl 2014. Nucleic Acids Res. 2014; 42:D749–55. [PubMed: 24316576]
51. Kent WJ, et al. The human genome browser at UCSC. Genome Res. 2002; 12:996–1006. [PubMed: 12045153]
52. Safran M, et al. GeneCards Version 3: the human gene integrator. Database (Oxford). 2010:baq020. 2010. [PubMed: 20689021]
53. Yang J, Lee SH, Goddard ME, Visscher PM. Genome-wide complex trait analysis (GCTA): methods, data analyses, and interpretations. Methods Mol Biol. 2013; 1019:215–236. [PubMed: 23756893]
54. Liu Y, et al. Serial analysis of gene expression (SAGE) in normal human trabecular meshwork. Mol Vis. 2011; 17:885–893. [PubMed: 21528004]
55. Liu Y, et al. Gene expression profile in human trabecular meshwork from patients with primary open-angle glaucoma. Invest Ophthalmol Vis Sci. 2013; 54:6382–6389. [PubMed: 24003086]

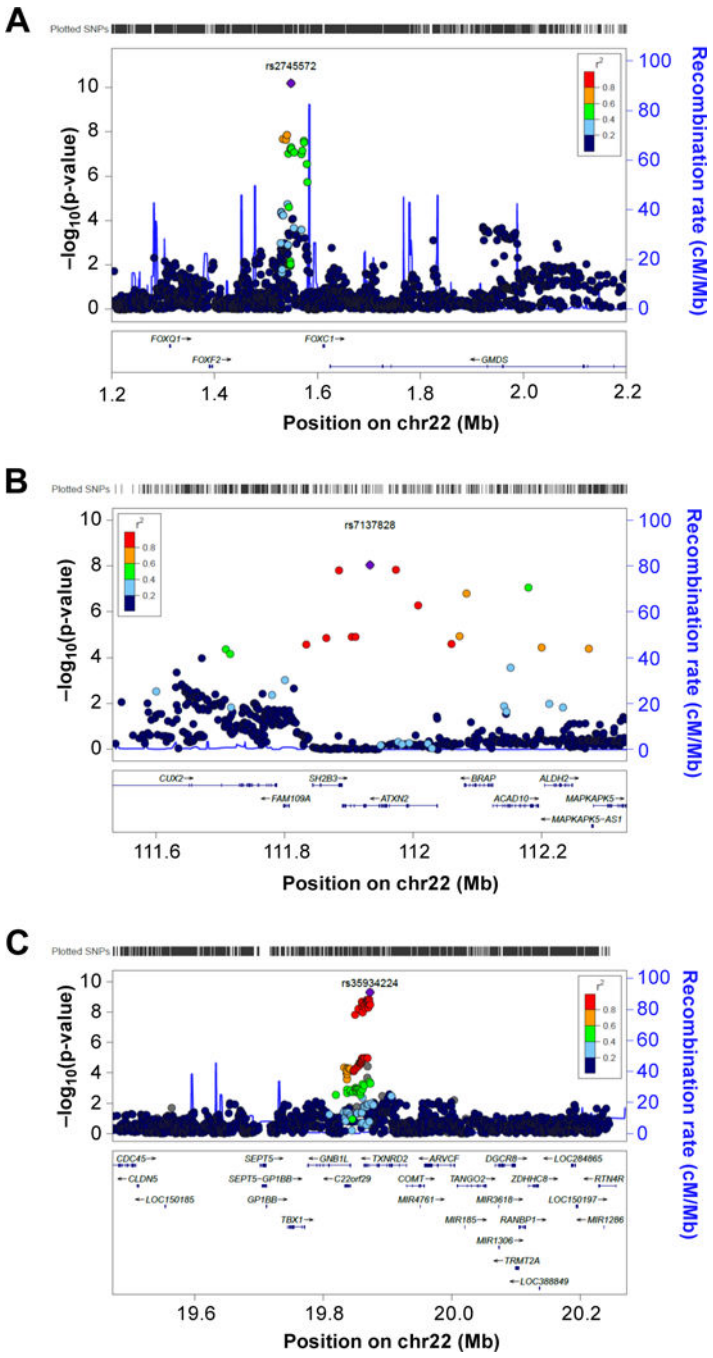

Figure 1. Association results for the regions reaching genome-wide significance after stage 2

These plots show the regional association and recombination rates for the top SNPs in the discovery cohort (NEIGHBORHOOD, 3,853 cases and 33,480 controls) after meta-analysis with data for these SNPs from ANZRAG (1,155 cases and 1,992 controls). In each plot, the solid diamond indicates the top-ranked SNP in the region based on two-sided P values. The colored box at the right or left corner of each plot indicates the pairwise correlation (r^2) between the top SNP and the other SNPs in the region. The blue spikes show the estimated recombination rates. The box underneath each plot shows the gene annotations in the region.

Each plot was created using LocusZoom for the top-ranked SNP in each region with a 400 kb region surrounding it. (a) The top SNP for this plot is rs2745572 on chromosome 6 upstream of *FOXC1* with $P = 6.50\times10^{-11}$. (b) The top SNP for this plot is rs7137828 on chromosome 12 within *ATXN2* with $P = 9.20\times10^{-9}$. (c) The top SNP for this plot is rs35934224 on chromosome 22 within *TXNRD2* with $P = 1.08\times10^{-9}$.

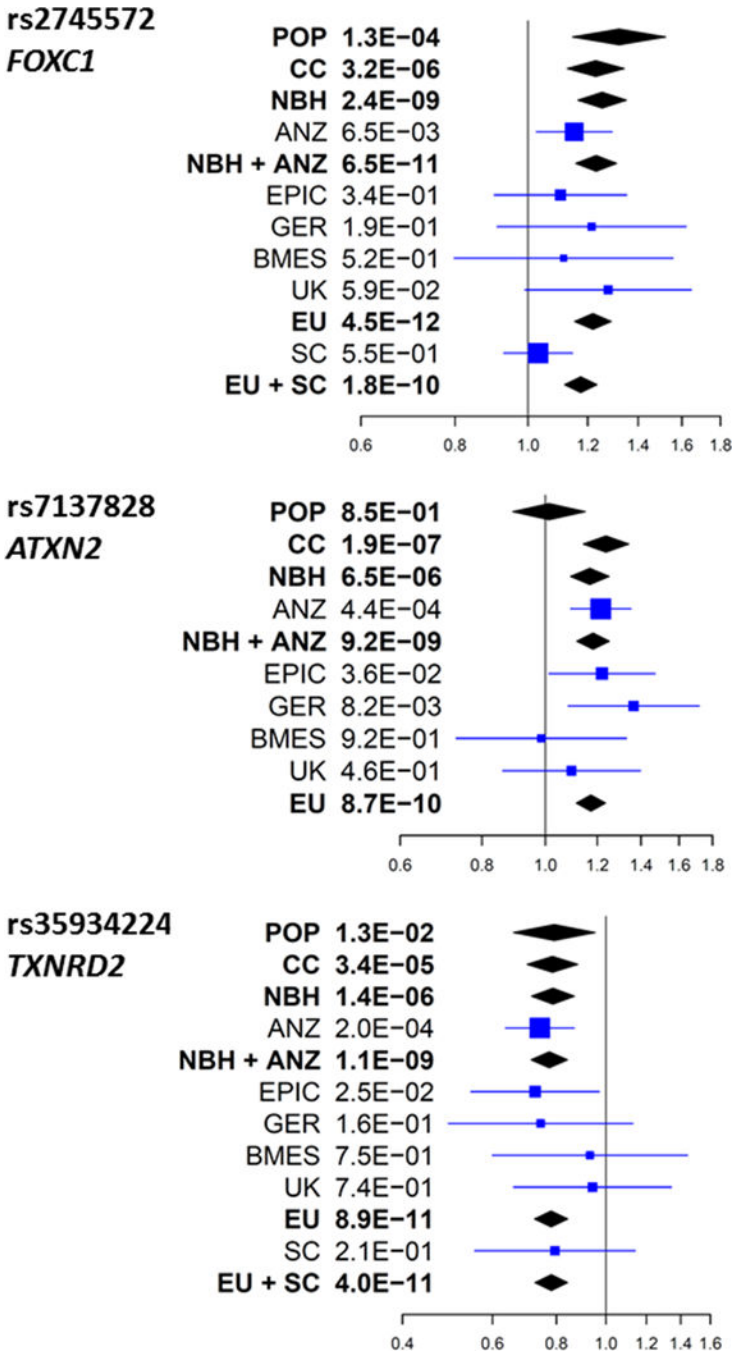

Figure 2. Meta-analysis Results

Forest plots showing effect estimates for participating studies, as well as for the replication effort. Pooled estimates for odds ratios and 95% confidence intervals were calculated by fixed effects, inverse variance weighting meta-analysis. Individual dataset results are indicated by blue squares and summary values are indicated by black diamonds. (Top) Association results for rs2745572 (*FOXC1* region top SNP). (Middle) Association results for rs7137828 (*ATXN2* region top SNP). (Bottom) Association results for rs35934224 (*TXNRD2* region top SNP). For the overall NEIGHBORHOOD (NBH), the summary value

for the population cohorts (POP; NHS/HPFS/WGHS) are presented separately from the case/control cohorts (CC; Iowa, OHTS (Ocular Hypertension Treatment Study), Marshfield, MEEI, NEIGHBOR). Results for the individual NBH datasets are shown in Supplementary Figure 4. Individual and summary results for Stage 2 (ANZ and ANZ+NBH) and Stage 3 cohorts (EPIC, GER, UK, BMES, SC) and summary points for all European ancestry (EU) datasets and all datasets (EU + SC) are shown. For rs7137828 replication could not be completed in SC due to rare minor allele frequency. Total sample size for rs2745572 and rs35934224 is 7,027 cases and 42,772 controls, and for rs7137828, 5,990 cases and 40,179 controls. Abbreviations: ANZ, ANZRAG;EPIC, European Prospective Investigation into Cancer-Norfolk Eye Study; GER, Germany; UK, United Kingdom; SC, Singapore Chinese; EU, European ancestry.

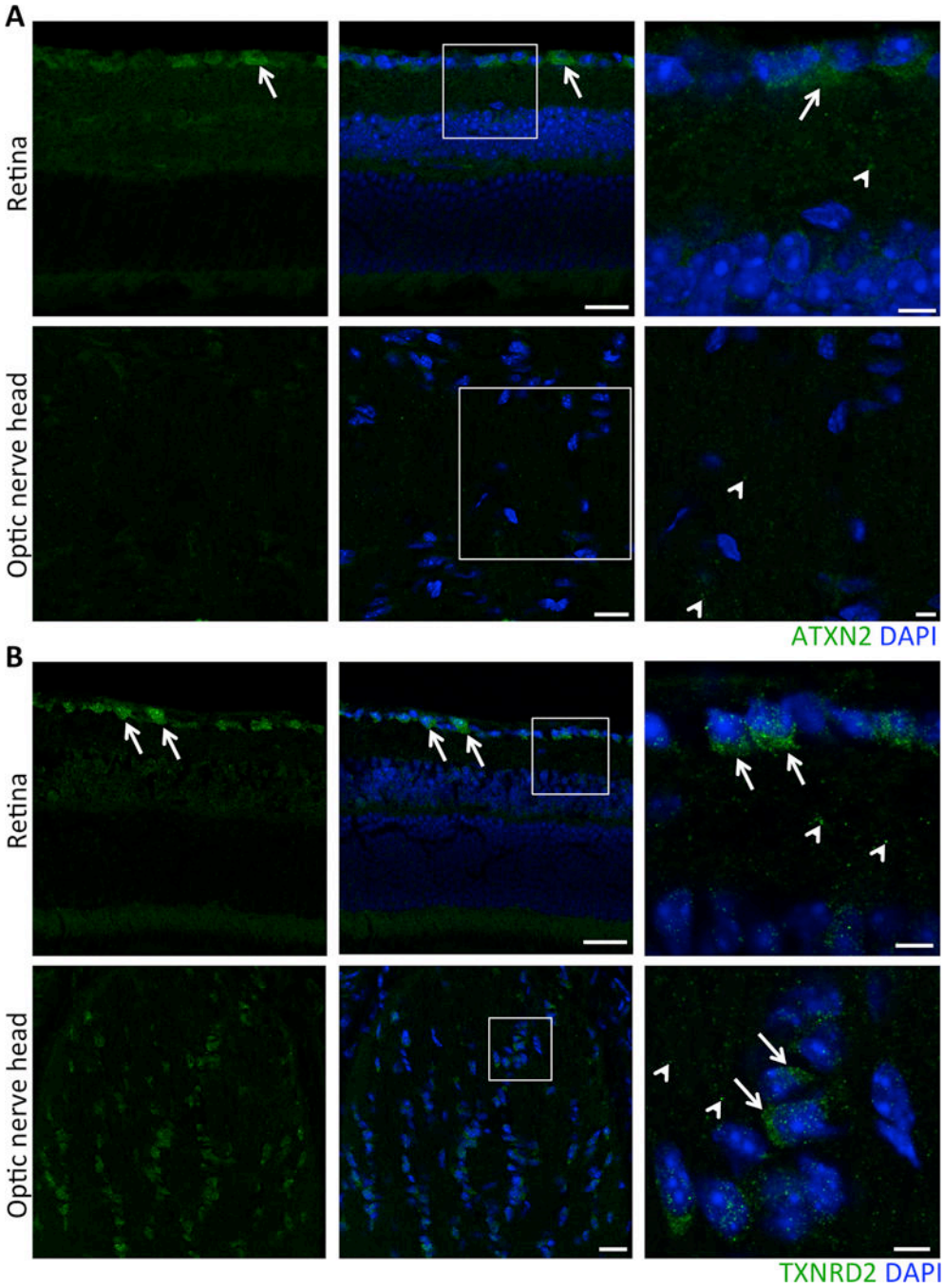

Figure 3. ATXN2 and TXNRD2 are expressed in the retina and optic nerve head

(A) Representative images of immunofluorescence using an anti-ATXN2 antibody shows ATXN2 (green) present in cells in the ganglion cell layer (arrows, upper panels) as well as punctate staining in the inner plexiform layer (arrowhead, right most upper panel). Only a low level of punctate staining was observed in the optic nerve head (arrowhead, lower panels). (B) Representative images of immunofluorescence using an anti-TXNRD2 antibody shows TXNRD2 (green) present in cells in the ganglion cell layer (arrows, upper panels) as well as significant punctate staining in the inner plexiform layer (arrowheads, right most

panel). Significant staining was also observed in cells in the optic nerve head (lower panels) indicative of astrocytes that form pial columns (arrows, right most panel). Punctate staining was also observed in the optic nerve head (arrowheads, lower panels). For each antibody, at least 3 sections from 6 eyes were assessed. No staining (not even punctate staining) was observed in the no primary control tissue (data not shown). Blue=DAPI. In all rows, right most panels are boxed regions in center panels. Scale bars: Upper left and center panels in A and B = 20 μm; Lower left and center panels in A = 15 μm; Lower left center and panels in B = 25 μm; Right most panels in A and B = 5 μm.

Table 1

Association and meta-analyses of the NEIGHBORHOOD and ANZRAG cohorts for the top-ranked loci.

						NEIGHBORHOOD (discovery, stage 1)		ANZRAG (replication, stage 2)		Meta-analysis NEIGHBORHOOD + ANZRAG			
Chr	**SNP**	**Position**	**A1**	**A2**	**Gene**	**OR**	**P**	**OR**	**P**	**OR**	**P**	**Het I^2**	**Het P**
1	rs7518099	165736880	t	c	*TMCO1*	0.70	3.12E-13	0.71	8.02E-06	0.70	6.35E-18	4.1	0.40
4	rs11732100	7924690	t	c	*AFAP1*	0.85	3.93E-06	0.78	6.77E-06	0.83	1.98E-10	24.1	0.23
6	**rs2745572**	**1548369**	**a**	**g**	***FOXC1***	**1.25**	**2.36E-09**	**1.18**	**6.46E-03**	**1.23**	**6.50E-11**	**0**	**0.58**
9	rs7866783	22056359	a	g	*CDKN2B-AS1*	0.70	1.04E-23	0.67	2.92E-12	0.69	1.22E-34	39.2	0.11
9	rs2472493	107695848	a	g	*ABCA1*	0.83	1.24E-07	0.70	2.08E-10	0.79	2.44E-15	34	0.15
12	**rs7137828**	**111932800**	**t**	**c**	***ATXN2***	**1.17**	**6.53E-06**	**1.22**	**4.36E-04**	**1.18**	**9.20E-09**	**3.1**	**0.41**
14	rs33912345	60976537	a	c	*SIX6*	0.76	8.94E-15	0.78	6.21E-06	0.76	1.71E-19	0	0.87
17	rs9897123	10020501	t	c	*GAS7*	0.85	6.86E-06	0.79	1.45E-05	0.83	5.85E-10	0	0.69
22	**rs35934224**	**19872645**	**t**	**c**	***TXNRD2***	**0.79**	**1.39E-06**	**0.74**	**2.01E-04**	**0.77**	**1.08E-09**	**0**	**0.83**

Association results for the SNPs reaching genome-wide significance in the discovery cohort (rs2745572) as well as other top-ranked loci showing replication. Genomic position is based on build 37. A1 is the effect allele for both cohorts. Novel loci are highlighted in bold font. Abbreviations: NEIGHBORHOOD, National Eye Institute Glaucoma Human Genetics Collaboration Heritable Overall Operational Database; ANZRAG, Australian and New Zealand Registry of Advanced Glaucoma; Chr, chromosome; OR, odds ratio; Het I^2, heterogeneity I^2 index; Het P, p-for-heterogeneity; N/A, not available. Loci not previously reported are denoted in bold text.